Available online at www.sciencedirect.com
ScienceDirect
Journal of the European Ceramic Society 31 (2011) 2741–2747
www.elsevier.com/locate/jeurceramsoc

Characterization of microstructural and thermal properties of steatite/cordierite ceramics prepared by using natural raw materials

Hasan Gökçe [a], Duygu Ağaoğulları [a,*], M. Lütfi Öveçoğlu [a], İsmail Duman [a], Tahsin Boyraz [b]

[a] *Istanbul Technical University, Faculty of Chemical and Metallurgical Engineering, Department of Metallurgical and Materials Engineering, 34469 Maslak, Istanbul, Turkey*

[b] *Cumhuriyet University, Faculty of Engineering, Department of Metallurgical and Materials Engineering, 58140 Campus, Sivas, Turkey*

Available online 31 December 2010

Abstract

Steatite/cordierite ceramics were fabricated by using a combined method of high-energy ball milling, cold pressing and sintering. Steatite and cordierite powders were separately synthesized from natural raw materials such as kaolinite and talc. The powder blends containing different amounts of cordierite (5, 10 and 20 wt.%) were wet-milled for 1 h in a vibratory ball-mill (Fritsch™ Pulverisette 7 Premium Line), using zirconia vial and balls. After drying, powders were compacted to cylindrical preforms with a diameter of 12.7 mm by uniaxial pressing at 300 MPa. The green compacts were sintered at 1200–1350 °C for 2 h under air. Phase, microstructural and thermal characterizations of the sintered materials were carried out by using X-ray diffraction technique (XRD), thermogravimetry/differential thermal analyzer (TG/DTA) and scanning electron microscope (SEM). Densities, open porosity and water absorption values of sintered bodies were measured by Archimedes method. Thermal expansion coefficient (CTE) measurements were conducted by a dilatometer.

Keywords: Silicates; Steatite/cordierite; Milling; Pressing; Sintering

1. Introduction

Steatite ceramics and cordierite ceramics are metasilicates which form the major components of the $MgO–Al_2O_3–SiO_2$ ternary system.[1] The chemical formula of steatite ceramics is $MgSiO_3$ which have four polymorphic forms such as enstatite, protoenstatite, clinoenstatite and high temperature clinoenstatite.[2,3] Steatite ceramics are usually available as an enstatite phase whose density is 3.21 g/cm^3, melting point is 1557 °C and crystal lattice is orthorhombic.[1] They are produced from natural raw materials as talc and clay by dry pressing, extrusion, casting and semi-wet pressing. Also, flux (BaO, $BaCO_3$, etc.) can be added at low quantities in order to improve the properties and distinguish the types of steatites.[4,5] The clay enhances the formability and processability of the body. The flux enables the development of a melting phase during sintering.[4]

Steatite ceramics are widely used in high temperature applications and electronics as tips for gas burners, heating element holders, halogen bulb holders, casings for thermostats, electric switchboards, stand off insulators, interlocking insulating beads, split bush insulators and regulator parts, due to their low dielectric losses, high temperature resistance and high mechanical strength. Moreover, they have been attracted considerable interest in dental applications.[2,4–8]

Cordierite ceramics contain $MgO:Al_2O_3:SiO_2$ ternary system components in the ratio of 2:2:5. Cordierite has an orthorhombic crystal lattice. Its density is 2.60 g/cm^3 and melting point is 1470 °C. They have superior properties such as excellent thermal shock resistance, low thermal expansion coefficient (CTE), high chemical durability, low dielectric constant and high refractoriness. Its mean CTE values vary with the cordierite content in the ceramic; typical values are 1.5×10^{-6} to 4.0×10^{-6} C^{-1} in the temperature range of 25–700 °C.[9–13] Steatite ceramics have higher CTE values (6×10^{-6} to 8×10^{-6} C^{-1}) than those of cordierite. Moreover, cordierite ceramics have higher thermal shock resistance than steatite.[1] On this basis, cordierite ceramics have many application areas as electrical porcelains, catalytic converter substrates for exhaust gas control of automobiles, heat exchangers for gas

* Corresponding author. Tel.: +90 212 285 6893; fax: +90 212 285 3427.
E-mail addresses: gokceh@itu.edu.tr (H. Gökçe), bozkurtdu@itu.edu.tr (D. Ağaoğulları), ovecoglu@itu.edu.tr (M.L. Öveçoğlu), iduman@itu.edu.tr (İ. Duman), tahsinboyraz@cumhuriyet.edu.tr (T. Boyraz).

0955-2219/$ – see front matter © 2010 Elsevier Ltd. All rights reserved.
doi:10.1016/j.jeurceramsoc.2010.12.007

turbine engines, industrial furnaces, packing materials in electronic packing, refractory coatings for metals, substrates for integrated circuits, etc.[11–16] Owing to their lower manufacturing costs and better electrical properties, cordierite ceramics are candidate materials instead of alumina, especially in the electronic industry.[1,9–11]

This study reports the fabrication of steatite/cordierite ceramics by using a combined method of high-energy ball milling, cold pressing and sintering. Steatite and cordierite powders were separately synthesized from natural raw materials such as kaolinite and talc. The effects of cordierite content (wt.%) and sintering temperature on the compositional, thermal, physical and microstructural features of the steatite/cordierite ceramics were evaluated.

2. Experimental procedure

The starting materials (steatite and cordierite) of this study were synthesized from natural raw materials. First of all, natural raw materials (talc and kaolinite) were calcined at 1000 °C for 2 h in a Protherm™ PLF 160/15 box furnace, with a heating and cooling rate of 20 °C/min. The chemical analysis of the natural materials performed by Thermo Scientific Niton™ XL3t X-ray fluorescence (XRF) analyzer is given in Table 1. Then, steatite was prepared by using talc (Sivas, Turkey), Al_2O_3 (Sulzer Metco™, 99.5% purity) and $BaCO_3$ (Alfa Aesar™, 99.8% purity) while cordierite was prepared from kaolinite (Balıkesir, Turkey), talc and Al_2O_3. Steatite and cordierite powders were, respectively, annealed at 1320 °C and 1250 °C for 2 h, with a heating and cooling rate of 20 °C/min. Cordierite powders in weight percentage of 5, 10 and 20% were added to the steatite powders. The addition amount of cordierite powder was not changed between 20 and 100 wt.% since cordierite acts as a reinforcement material in the steatite matrix and when its positive effect was observed, the experiments were terminated. The powder blends were wet-milled in ethanol (Merck™, 96% purity) for 1 h by using Fritsch™ Pulverisette 7 Premium Line with a rotation speed of 800 rpm. Milling experiments were carried out using zirconia balls (diameter: 10 mm) in a zirconia vial (80 ml) with a ball-to-powder weight ratio (BPR) of 8:1. Then, powder blends were dried in a Heraeus™ stove at 80 °C for 24 h. In order to understand the effect of milling on the starting powders, particle size distributions of steatite and cordierite were determined by a Malvern™ Mastersizer 2000 particle analyzer before and after milling. After drying, 2 wt.% binder agent (polyvinyl alcohol) was added to the powder blends and they were compacted in a 10 ton capacity MSE™ MP-0710 uni-action hydraulic press to obtain cylindrical preforms with a diameter of 12.7 mm under an uniaxial pressure of 300 MPa. The green compacts were sintered at the temperatures between 1200 °C and 1350 °C for 2 h in a Protherm™ PLF 160/15 box furnace, with a heating and cooling rate of 20 °C/min under air. The sintered samples were assigned as S, SC5, SC10, SC20 and C, according to the content of cordierite 0, 5, 10, 20 and 100 wt.%, respectively.

Table 1
Chemical analysis of the natural raw materials.

	Composition (wt.%)	
	Talc	Kaolinite
SiO_2	63.7	48.6
Al_2O_3	0.07	35.6
Fe_2O_3	0.41	0.8
TiO_2	–	0.1
MgO	30.25	–
CaO	0.22	2.9
Ignition loss	5.35	12

The phase compositions of the raw materials and sintered bodies were performed by X-ray diffraction (XRD) technique using a Bruker™ D8 Advanced Series powder diffractometer with Cu Kα (1.54060 Å) radiation in the 2θ range of 8–80° with 0.02° steps at a rate of 2°/min. The International Centre for Diffraction Data® (ICDD) powder diffraction files were utilized for the identification of crystalline phases. Thermal property of the selected powder blend was conducted in an alumina crucible heated up to 1000 °C with 10 °C/min under air, by using a PerkinElmer™ Diamond thermogravimetry/differential thermal analyzer (TG/DTA). Microstructural characterizations of the sintered bodies were carried out using a Hitachi™ TM-1000 scanning electron microscope (SEM) operated at 15 kV. Density, porosity and water absorption values of the sintered bodies were measured by Archimedes method. The results were reported as the arithmetic means of measurements taken from three different samples. Thermal expansion coefficient measurements were performed by using a Unitherm™ 1161 V high-temperature vertical dilatometer heated up to 1000 °C with 10 °C/min under air.

3. Results and discussion

The XRD patterns of the steatite and cordierite powders annealed at 1320 °C and 1250 °C for 2 h are illustrated in Fig. 1(a) and (b). Steatite powders contain clinoenstatite (ICDD Card No: 084-0652, Bravais lattice: primitive monoclinic, $a = 0.96$ nm, $b = 0.881$ nm, $c = 0.517$ nm) and protoenstatite (ICDD Card No: 074-0816, Bravais lattice: primitive orthorhombic, $a = 0.925$ nm, $b = 0.874$ nm, $c = 0.532$ nm) phases according to Fig. 1(a). Fig. 1(b) illustrates that annealed cordierite powders have cordierite (ICDD Card No: 012-0303, Bravais lattice: base-centered orthorhombic, $a = 0.974$ nm, $b = 1.708$ nm, $c = 0.935$ nm), indialite (ICDD Card No: 048-1600, Bravais lattice: primitive hexagonal, $a = b = 0.977$ nm, $c = 0.937$ nm), mullite (ICDD Card No: 015-0776, Bravais lattice: primitive orthorhombic, $a = 0.755$ nm, $b = 0.769$ nm, $c = 0.288$ nm), magnesium silicate (ICDD Card No: 011-0273, Bravais lattice: primitive orthorhombic, $a = 0.925$ nm, $b = 0.874$ nm, $c = 0.532$ nm) and corundum (ICDD Card No: 046-1212, Bravais lattice: primitive rhombohedral, $a = b = 0.476$ nm, $c = 0.130$ nm) phases. The effect of milling on steatite and cordierite powders was obviously seen in Figs. 2 and 3. Milling provides decrease in the average particle size of steatite from 32.289 μm to 7.623 μm and cordierite from 33.049 μm to 7.439 μm. In order to understand the thermal behaviour of the wet-milled

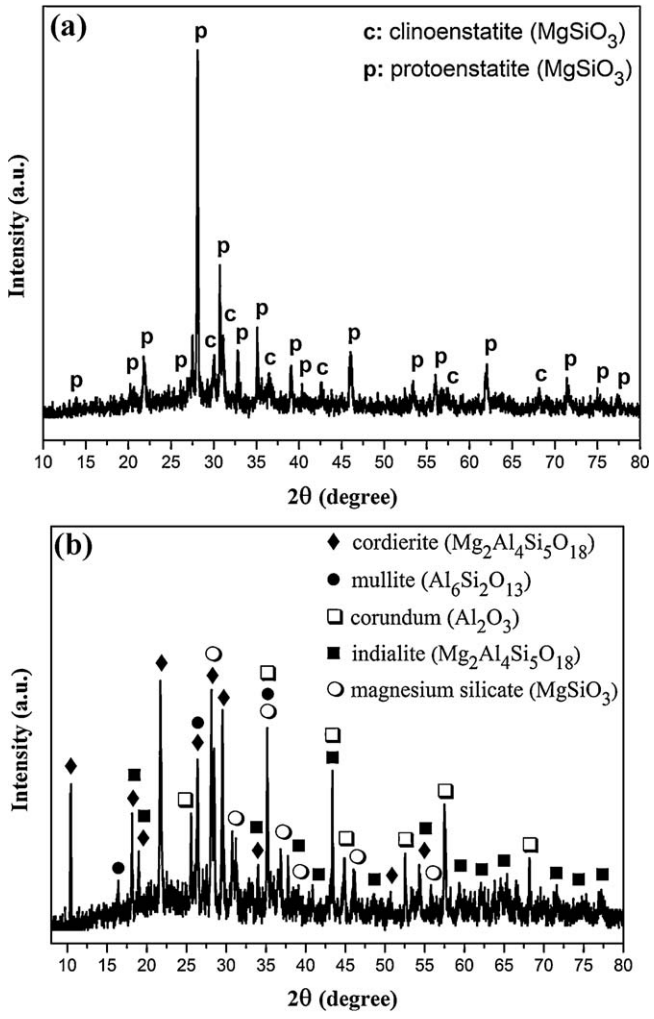

Fig. 1. The XRD patterns of the annealed steatite (a) and cordierite (b) powders.

and dried steatite/cordierite powder blends before sintering, thermogravimetry/differential thermal analysis (TG/DTA) was performed on the steatite–10 wt.% cordierite powder blend. DTA curve of the powder blend given in Fig. 4(a) illustrates that clear

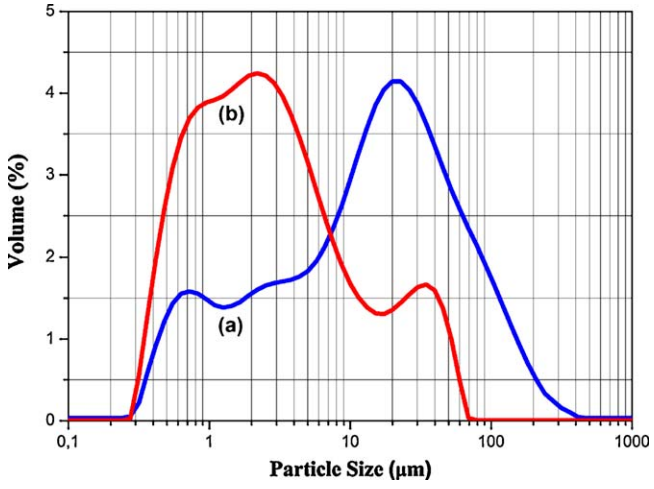

Fig. 2. Particle size distributions of steatite powders: (a) before milling and (b) after milling.

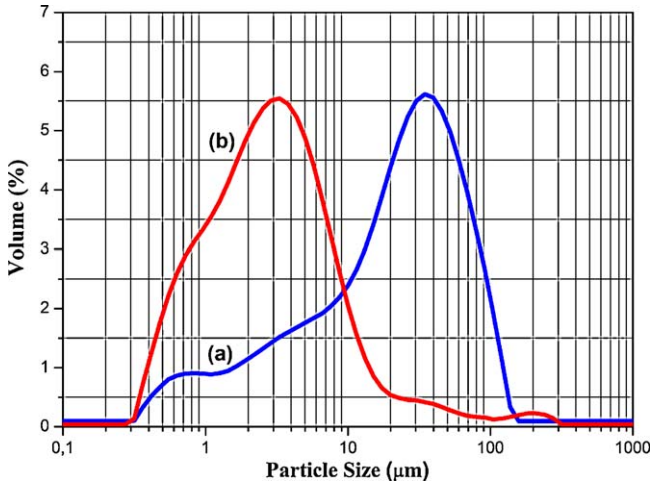

Fig. 3. Particle size distributions of cordierite powders: (a) before milling and (b) after milling.

endothermic and/or exothermic peaks do not appear during heating to 1000 °C. According to the TG curve shown in Fig. 4(b), there is not a considerable weight gain or weight loss, which it coincides that there is no interaction between steatite and cordierite ceramics up to 1000 °C. On the basis of Fig. 4(a) and (b), sintering process was carried out above 1000 °C and the lower limit of the sintering was selected as 1200 °C to ensure the interaction.

Fig. 5 represents the XRD patterns of the S, SC5, SC10, SC20 and C samples at 1200 °C. There are clinoenstatite and protoenstatite phases in the S, SC5, SC10 and SC20 samples. SC5, SC10 and SC20 samples also have small amount of forsterite (ICDD Card No: 034-0389, Bravais lattice: primitive orthorhombic, $a = 0.598$ nm, $b = 1.020$, $c = 0.475$ nm) phase which arises from the partial decomposition of cordierite in the composition. However, forsterite ($2MgO{\cdot}SiO_2$) phase is more distinctive in SC10 and SC20 samples. Figs. 6 and 7 show the XRD patterns of the S, SC5, SC10, SC20 and C samples at 1300 and 1350 °C, respectively. The XRD patterns of the samples are almost the same with each other. In addition to clinoenstatite, protoenstatite, cordierite and forsterite phases, very small amount of

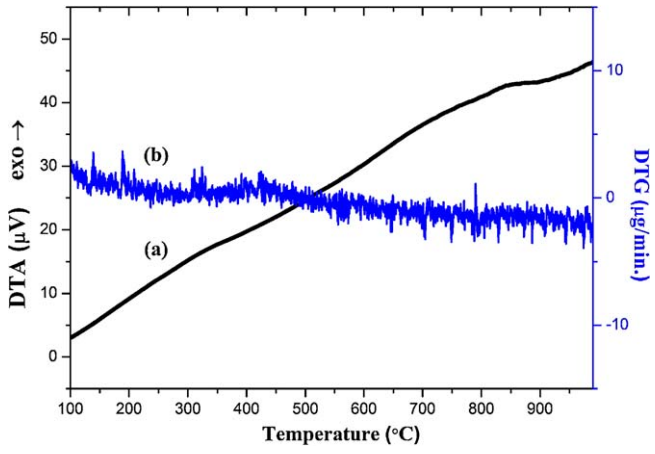

Fig. 4. TG/DTA analysis of steatite–10 wt.% cordierite powder blend: (a) DTA curve and (b) TG curve.

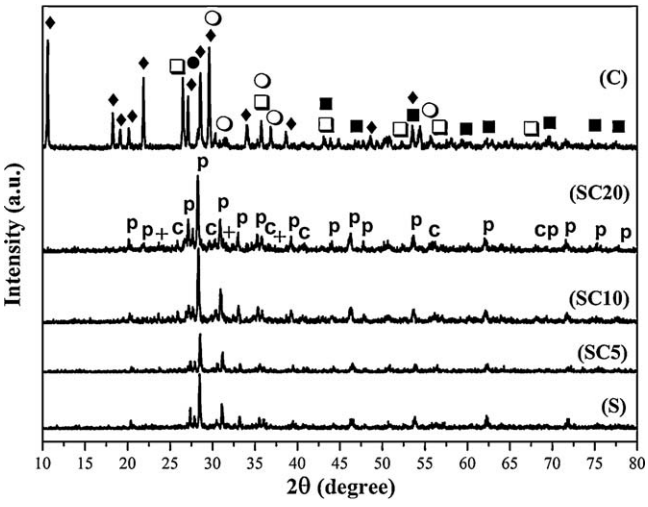

Fig. 5. The XRD patterns of the S, SC5, SC10, SC20 and C samples sintered at 1200 °C. (p: protoenstatite, c: clinoenstatite, +: forsterite, ♦: cordierite, □: corundum, ●: mullite, ◯: magnesium silicate and ■: indialite).

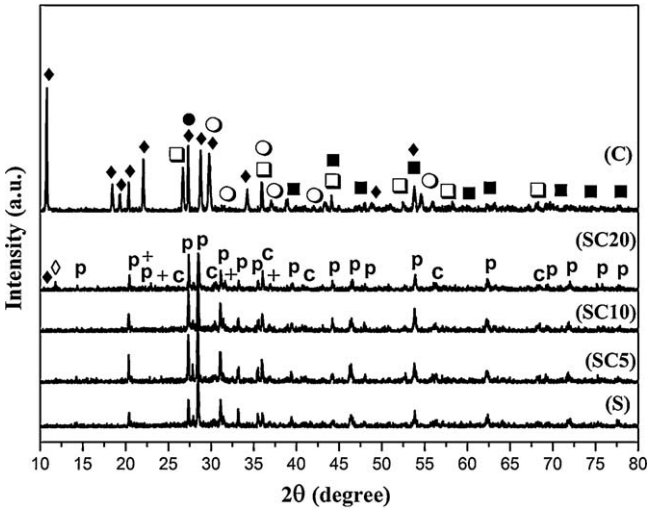

Fig. 7. The XRD patterns of the S, SC5, SC10, SC20 and C samples sintered at 1350 °C. (p: protoenstatite, c: clinoenstatite, +: forsterite, ♦: cordierite, □: corundum, ●: mullite, ◯: magnesium silicate, ■: indialite and ◊: SiO_2).

SiO_2 (ICDD Card No: 051-1382, Bravais lattice: body-centered orthorhombic, $a = 1.367$ nm, $b = 0.502$ nm, $c = 2.556$ nm) phase occur in the SC5, SC10 and SC20 samples. Moreover, this phase is clearer in SC20. It can be explained as appearance of SiO_2 during partial decomposition of cordierite in order to form forsterite.

Table 2 illustrates the physical properties (density, porosity and water absorption) of the sintered steatite–x wt.% cordierite ($x = 5$, 10 and 20) ceramics. Sintered steatite and sintered cordierite were separately present in Table 2 in order to determine the effect of cordierite addition on the physical properties of steatite-based ceramics. It should be noted that the porosity measurements of the samples were valid for open pores. In the scope of this study, it is not aimed to determine the closed pores. Table 2 shows that relative density has a descending tendency up to 20 wt.% cordierite content, for all sintering temperatures (1200, 1300 and 1350 °C). Cordierite addition has a negative effect on the relative density of the steatite-based ceramics (SC5 and SC10) until its content reaches to 20 wt.%. There is an increase in the relative density of the SC20 at all sintering temperatures. However, this increase is sharper for the temperatures of 1300 and 1350 °C. Furthermore, at all sintering temperatures, SC20 has higher relative density than sintered steatite. The relative density values of all sintered samples increase as sintering temperature increases. This is not a surprising phenomenon because the annealing temperature of 1300 and 1350 °C are closer to the melting point of starting materials and partial melting can occur to form denser bodies. As seen in Table 2, porosity and water absorption values increase up to the cordierite content of 20 wt.%, inversely to the

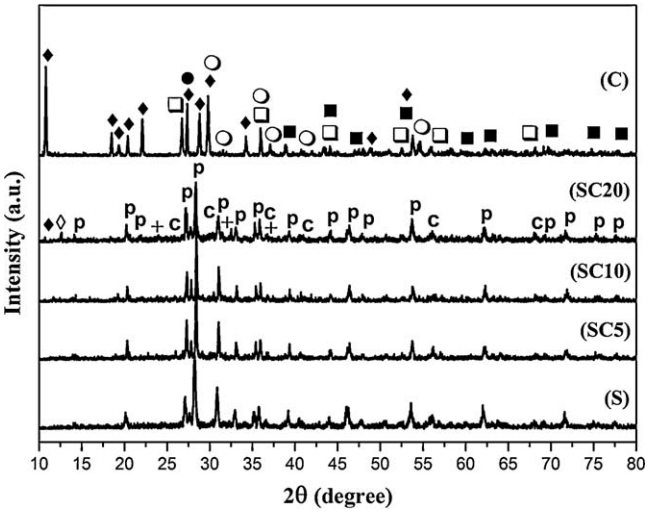

Fig. 6. The XRD patterns of the S, SC5, SC10, SC20 and C samples sintered at 1300 °C. (p: protoenstatite, c: clinoenstatite, +: forsterite, ♦: cordierite, □: corundum, ●: mullite, ◯: magnesium silicate, ■: indialite and ◊: SiO_2).

Table 2
Physical properties of the sintered steatite/cordierite ceramics.

	ρ_{bulk} (g/cm^3)	ρ_{true} (g/cm^3)	$\rho_{relative}$ (%)	Porosity (%)	W. Abs. (%)
1200 °C					
S	2.27	3.21	70.72	27.13	11.95
SC5	2.21	3.18	69.49	28.50	12.80
SC10	2.18	3.15	69.20	28.60	12.90
SC20	2.19	3.09	70.87	26.95	10.87
C	1.95	2.60	75.00	28.05	14.58
1300 °C					
S	3.00	3.21	93.45	0.63	0.15
SC5	2.96	3.18	93.08	0.72	0.21
SC10	2.90	3.15	92.10	0.86	0.30
SC20	2.94	3.09	95.15	0.08	0.07
C	2.25	2.60	86.53	12.70	5.60
1350 °C					
S	3.10	3.21	96.57	0.40	0.10
SC5	3.02	3.18	94.97	0.56	0.17
SC10	2.92	3.15	92.70	0.65	0.22
SC20	2.99	3.09	96.76	0.02	0.03
C	2.55	2.60	98.08	0.98	0.38

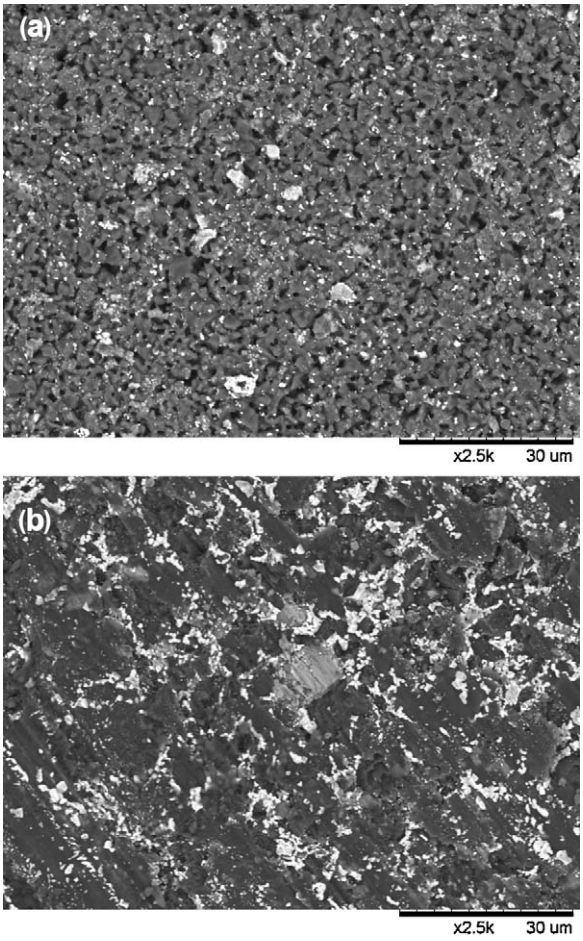

Fig. 8. SEM images of the S sample sintered at: (a) 1200 °C and (b) 1350 °C.

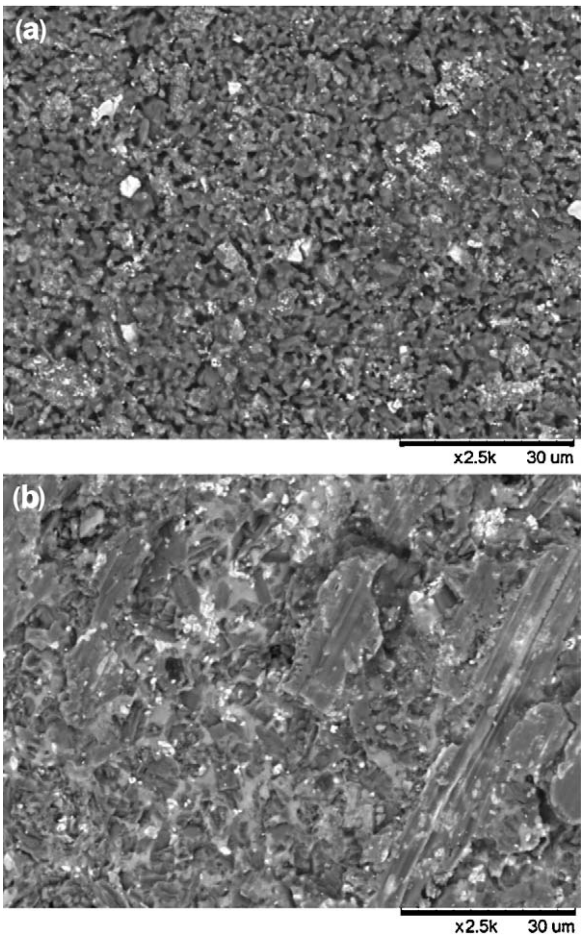

Fig. 9. SEM images of the SC20 sample sintered at: (a) 1200 °C and (b) 1350 °C.

relative density values. It is evident from Table 2 that porosity and water absorption values decrease as sintering temperature increases. It can be concluded that it is possible to produce fully dense steatite/cordierite ceramics with low porosity and water absorption values from natural raw materials, above 1350 °C. However, the lower content of cordierite should be 20 wt.% considering the increase in relative density and the decrease in porosity and water absorption. Moreover, it is obviously understood that XRD pattern of SC20 at 1350 °C supports the obtained values given in Table 2. Due to the fact that there is a reaction between cordierite and steatite to form forsterite, the highest relative density and the lowest porosity and water absorption values were obtained for SC20 coinciding a denser body.

Fig. 8(a) and (b) are the SEM images of the S sample sintered at 1200 and 1350 °C, respectively. SEM image of S sintered at 1200 °C has a very porous body as compatible with the XRD patterns and physical properties defined in Table 2. As temperature increases to 1350 °C, the body becomes denser but in a segmentary appearance. Fig. 9(a) and (b) are the SEM images of the SC20 sample sintered at 1200 and 1350 °C, respectively. As seen in these figures, porous body of the SC20 becomes denser as sintering temperature increases, with the assistance of reaction taking place between steatite and cordierite. Cordierite particles embedded in the steatite matrix have homogeneous distribution throughout the structure. However, there is not a significant difference between the SEM images of S and SC20 since Table 2 gives closer relative density values for these two samples at both sintering temperatures. The SEM images of the samples are compatible with the current literature.[2,5]

Fig. 10(a)–(c) demonstrates the linear thermal expansion coefficients (CTE) of S, SC5, SC10, SC20 and C samples for 1200, 1300 and 1350 °C. Although literature data respectively gives the CTE values of steatite and cordierite as 6×10^{-6} to $8 \times 10^{-6}\,C^{-1}$ and 1.5×10^{-6} to $4 \times 10^{-6}\,C^{-1}$, CTE of steatite was found in the range of 4×10^{-6} to $6 \times 10^{-6}\,C^{-1}$ and CTE of cordierite was determined in the range of 10×10^{-6} to $11 \times 10^{-6}\,C^{-1}$, according to Fig. 10(a)–(c). As clearly seen in these figures, the addition of cordierite decreases the CTE values of steatite-based ceramics for all sintering temperatures. The lowest CTE value was obtained in SC20 sample in the range of 7.25×10^{-6} to $9.5 \times 10^{-6}\,C^{-1}$. The addition of cordierite causes a decrease in CTE values at about 25%. Thus, the most important effect of the cordierite on steatite emerges in the CTE values. It is well known that a low CTE is one of the requirements for improving thermal shock resistance of ceramics at elevated temperatures.

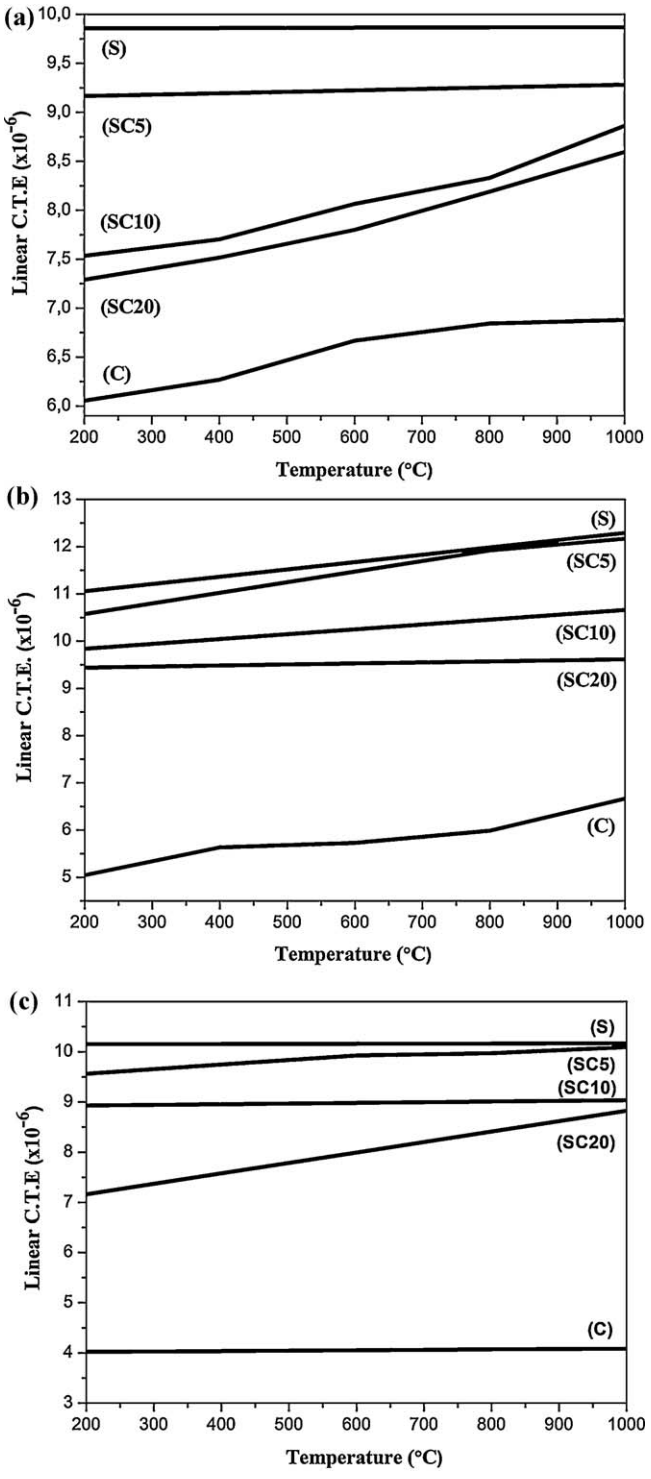

Fig. 10. The linear thermal expansion coefficients of S, SC5, SC10, SC20 and C samples for sintering temperatures of: (a) 1200 °C, (b) 1300 °C and (c) 1350 °C.

4. Conclusions

Based on the results of the present study, the following conclusions can be drawn:

1. Clinoenstatite, protoenstatite, cordierite and forsterite phases in addition to very small amount of SiO_2 phase occur in the SC5, SC10 and SC20 samples at 1300 and 1350 °C. However, this phase is clearer in SC20. It can be explained with the partial decomposition of cordierite and reaction with steatite in order to form forsterite.
2. The relative density values of all sintered samples increase as sintering temperature increases.
3. Cordierite addition has a negative effect on the relative densities of the steatite-based ceramics until its content reaches to 20 wt.%.
4. The highest relative density and so the lowest porosity and water absorption values were obtained in SC20 sample at 1350 °C.
5. SEM images prove that porous bodies of the steatite/cordierite ceramics become denser as sintering temperature increases.
6. CTE values of steatite/cordierite ceramics decrease as cordierite content (wt.%) increases, for all sintering temperatures. The lowest CTE value was obtained in SC20 ceramic in the range of 7.25×10^{-6} to 9.5×10^{-6} C^{-1}.

Acknowledgements

This study is one of the outcomes of a research project entitled "Development of Al–Cu Based Metal Matrix Composites via Powder Metallurgy Techniques" funded by State Planning Organization (DPT) with the project number 90189. Further, we would like to express our gratitude to State Planning Organization (DPT) for funding the project entitled "Advanced Technologies in Engineering" with the project number 2001K120750 out of which the main infrastructure of the Particulate Materials Laboratories was founded.

References

1. Rohan P, Neufuss K, Matějíček J, Dubský J, Prchlík L, Holzgartner C. Thermal and mechanical properties of cordierite, mullite and steatite produced by plasma spraying. *Ceramics International* 2004;**30**:597–603.
2. Mielcarek W, Nowak-Woźny D, Prociów K. Correlation between $MgSiO_3$ phases and mechanical durability of steatite ceramics. *Journal of the European Ceramic Society* 2004;**24**:3817–21.
3. Reynard B, Bass JD, Jackson JM. Rapid identification of steatite–enstatite polymorphs at various temperatures. *Journal of the European Ceramic Society* 2008;**28**:2459–62.
4. Soykan HŞ. Low-temperature fabrication of steatite ceramics with boron oxide addition. *Ceramics International* 2007;**33**:911–4.
5. Vela E, Peiteado M, García F, Caballero AC, Fernández JF. Sintering behaviour of steatite materials with barium carbonate flux. *Ceramics International* 2007;**33**:1325–9.
6. Steatite gas-burners. *Journal of the Franklin Institute* 1859;**67**:125–6.
7. On the uses of steatite; and particularly in the lubrication of machinery to reduce friction. *Journal of the Franklin Institute* 1830;**9**:274–7.
8. On the uses of steatite. *Journal of the Franklin Institute* 1838;**25**:197–8.
9. Kobayashi Y, Sumi K, Kato E. Preparation of dense cordierite ceramics from magnesium compounds and kaolinite without additives. *Ceramics International* 2000;**26**:739–43.
10. Gökçe H, Öveçoğlu ML, Aslanoğlu Z, Özkal B. Microstructural characterization of cordierite ceramics produced from natural raw materials and synthetic powders. *Key Engineering Materials* 2004;**264–268**:1035–8.
11. Gökçe H, Öveçoğlu ML, Özkal B. Comparison of physical and mechanical properties of cordierite based ceramics produced from natural raw materials and synthetic powders. *Key Engineering Materials* 2004;**264–268**:929–32.

12. Goren R, Ozgur C, Gocmez H. The preparation of cordierite from talc, fly ash, fused silica and alumina mixtures. *Ceramics International* 2006;**32**:53–6.
13. Cameruccia MA, Urretavizcaya G, Cavalieri AL. Sintering of cordierite based materials. *Ceramics International* 2003;**29**:159–68.
14. Camerucci MA, Urretavizcaya G, Cavaliari AL. Mechanical behaviour of cordierite and cordierite-mullite materials evaluated by indentasyon techniques. *Journal of the European Ceramic Society* 2001;**21**:1195–204.
15. Costa Oliveira FA, Cruz Fernandes J. Mechanical and thermal behaviour of cordierite–zirconia composites. *Ceramics International* 2002;**28**:79–91.
16. Ghitulica C, Andronescu E, Nicola O, Dicea A, Birsan M. Preparation and characterization of cordierite powders. *Journal of the European Ceramic Society* 2007;**27**:711–3.